Functionalized 3D Polyurethane Foams with Microwave-synthesized TiO_2 Nanostructures for Solar Light-driven Degradation of Tetracycline

Maria Leonor Matias[1], Ana Pimentel[1], Ana S. Reis Machado[1,2], Joana Rodrigues[3], Auguste Fernandes[4], Teresa Monteiro[3], Patrícia Almeida Carvalho[5,6], Mariana N. Amaral[7,8], Catarina Pinto Reis[7,8], Jonas Deuermeier[1], Elvira Fortunato[1], Rodrigo Martins[1*], Daniela Nunes[1*]

[1]CENIMAT|i3N, Department of Materials Science, School of Science and Technology, NOVA University Lisbon and CEMOP/UNINOVA, 2829-516 Caparica, Portugal
[2]LAQV-REQUIMTE, Department of Chemistry, NOVA School of Science and Technology, Universidade NOVA de Lisboa, Campus de Caparica, 2829-516 Caparica, Portugal
[3]Physics Department and i3N, Aveiro University, Campus Universitário de Santiago, 3810-193 Aveiro, Portugal
[4]Centro de Química Estrutural, Instituto Superior Técnico, Universidade de Lisboa, Av. Rovisco Pais, 1049-001 Lisboa, Portugal
[5]SINTEF, Material Physics, 0373 Oslo, Norway
[6]CeFEMA, Instituto Superior Técnico, Universidade de Lisboa, Av. Rovisco Pais, 1049-001 Lisboa, Portugal
[7]Research Institute for Medicines (iMed.ULisboa), Faculty of Pharmacy, Universidade de Lisboa, Av. Professor Gama Pinto, 1649-003 Lisboa, Portugal
[8]Instituto de Biofísica e Engenharia Biomédica (IBEB), Faculdade de Ciências, Universidade de Lisboa, Campo Grande, 1749-016 Lisboa, Portugal

1. Experimental procedure

The standard curve of the TC solution is depicted in Figure S1. The linear expression that relates absorbance and concentration is given by the following equation:

$$A = 0.03705 \times C_{TC} \quad \text{(eq. S1)}$$

where A is the absorbance and C_{TC} is the TC concentration in $mg.L^{-1}$.

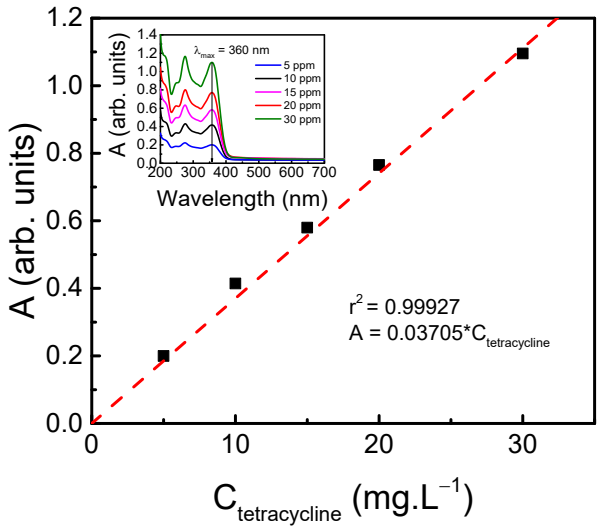

Figure S1 - Standard curve of tetracycline (TC). Inset: Absorbance spectra of different concentrations (5, 10, 15, 20 and 30 ppm) of TC.

2. Structural characterization of the TiO_2 nanopowders

Figure S2 shows TiO_2 anatase nanocrystals synthesized with ethanol as solvent. It is clear the presence of faceted nanocrystals. An individual TiO_2 faceted nanocrystal was observed using atomic-resolution STEM imaging, and a lattice spacing of 0.19 nm can be observed, which perfectly matches the (200) and (020) atomic planes of anatase [1]. Observed along the $[00\bar{1}]$ zone axis, it is evident from the FFT pattern that the angle between (200) and (020) is 90º, in accordance with the theoretical value reported for pure crystalline TiO_2 anatase (ICSD file no. 9852). In this material, low-index faceted nanocrystals and defective high-index nanocrystals were observed.

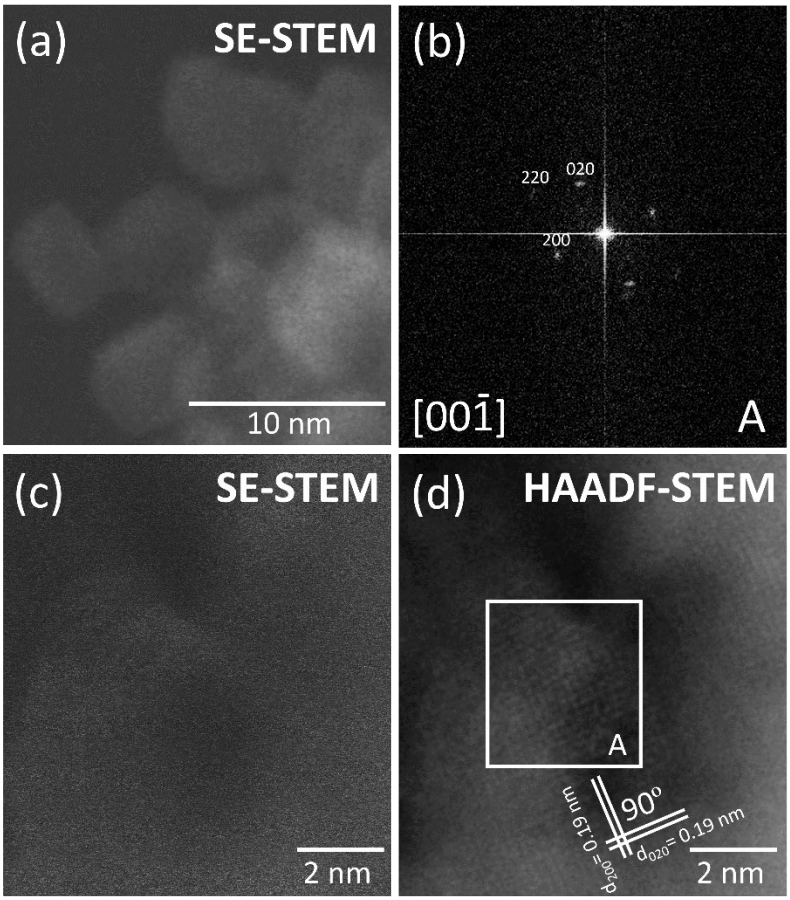

Figure S2 - (a) SE-STEM image of the TiO_2 anatase nanocrystals synthesized with ethanol, (b) FFT image obtained from the white square in (d), (c) and (d) SE-STEM and HAADF-STEM images of a low-index TiO_2 anatase faceted nanocrystal.

Figure S3 shows the survey spectra of all synthesized TiO_2 nanopowders.

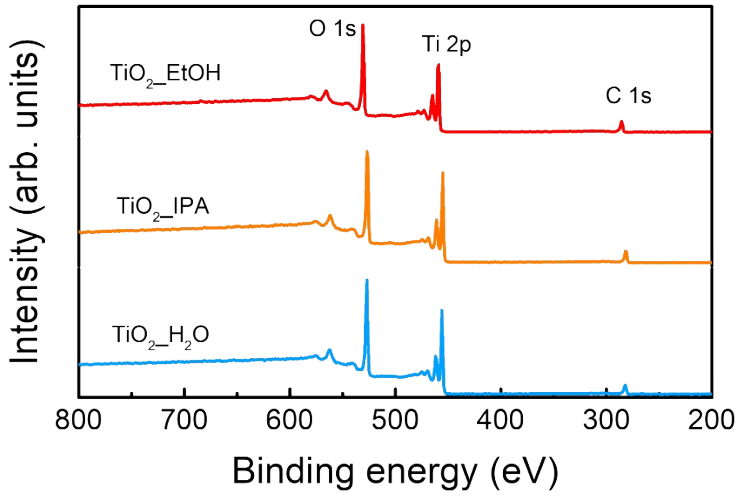

Figure S3 - Survey spectra of all synthesized TiO_2 nanopowders (TiO_2_EtOH, TiO_2_IPA, TiO_2_H_2O).

Figure S4 shows the normalized intensity of all XPS O 1s emissions. The TiO_2 nanocrystals synthesized with water clearly show a smaller intensity in the binding energy range of the surface oxygen component.

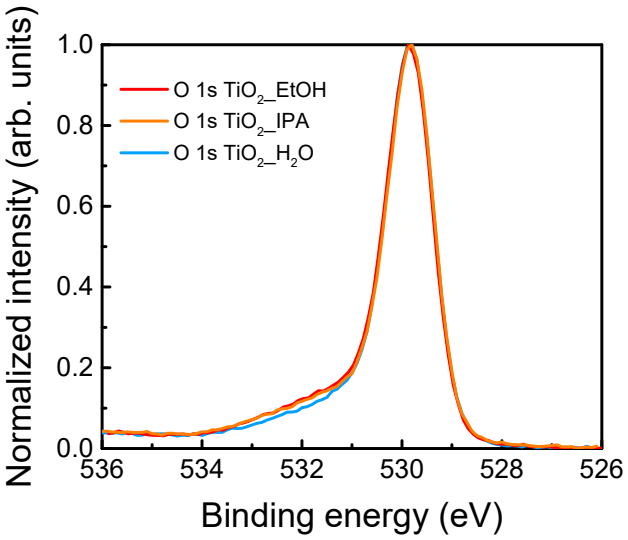

Figure S4 - Normalized intensity of all XPS O 1s emissions. The O 1s emissions in red, orange, and blue colors represent the TiO_2_EtOH, TiO_2_IPA and TiO_2_H_2O nanopowders, respectively.

3. Adsorption studies and adsorption kinetic models

The amount of adsorbed tetracycline per gram of adsorbent, and adsorption capacity (uptake, q ($mg.g^{-1}$)) was calculated according to eq. S2.

$$q = \frac{V.(C_0 - C_e)}{W} \times 100 \qquad \text{(eq. S2)}$$

In equation S2, C_0 and C_e are the initial and equilibrium concentrations of tetracycline ($mg.\ L^{-1}$), respectively, V is the volume of the solution (L), and W is the mass of the adsorbent (g) [2]. The percentage of pollutant uptake by the sorbent (sorption efficiency) was calculated using the following equation, eq. S3 [2]:

$$Sorption\ efficiency\ (\%) = \frac{C_0 - C_f}{C_0} \times 100 \qquad \text{(eq. S3)}$$

where C_0 and C_f are the initial and equilibrium concentrations of pollutant ($mg.L^{-1}$), respectively, after 180 min (4 h).

The pseudo-first order model given by Lagergren is described by the following equation [2]:

$$\log(q_e - q) = \log q_e - k_1 t/2.303 \qquad \text{(eq. S4)}$$

in which q_e and q represent the amounts of pollutant adsorbed (mg.g^{-1}) at the equilibrium time and time t (min) respectively, k_1 is the rate constant of sorption (min^{-1}). The rate constant and the corresponding linear regression correlation coefficient values can be determined from the straight-line plots of $\log(q_e - q)$ as a function of t [2].

The pseudo-second order model given by McKay and Ho is expressed by eq. S5 [2]:

$$\frac{t}{q} = \frac{1}{k_2 q_e^2} + \frac{t}{q_e} \quad \text{(eq. S5)}$$

where q_e and q represent the amounts of pollutant adsorbed (mg.g^{-1}) at the equilibrium time and time t (min) respectively, k_2 is the pseudo-second order rate constant (g.mg^{-1}. min^{-1}). The values of q_e and k_2 can be determined from the straight-line plots of $\frac{t}{q}$ as a function of t [2].

The linear form of the Elovich equation is represented by eq. S6 [2]:

$$q = \frac{ln(a_e b_e)}{b_e} + \frac{1}{b_e} ln(t) \quad \text{(eq. S6)}$$

in which a_e is the initial sorption rate constant (mg. g^{-1}. min^{-1}), b_e is related to the extent of surface coverage and the activation energy for chemisorption (g.mg^{-1}). The values of a_e and b_e can be obtained from the plot of q as a function of $ln(t)$ [2].

The intraparticle diffusion (Weber-Morris) model is expressed as [2]:

$$q = k_{id}\sqrt{t} + C \quad \text{(eq. S7)}$$

where k_{id} is the intraparticle diffusion rate constant (mg. g^{-1}. $min^{-0.5}$). If intraparticle diffusion occurs, then the plot of q against √t is linear. The value of the intercept (C) is related to the thickness of the boundary layer i.e., the larger the intercept the higher the boundary layer effect [2].

Bangham's model equation can be expressed by eq. S8 [2,3]:

$$loglog\left(\frac{C_0}{C_0 - qM}\right) = \log\left(\frac{k_b M}{2.303V}\right) + \alpha.log(t) \quad \text{(eq. S8)}$$

where C_0 is the initial concentration of the adsorbate in solution (mg.L^{-1}), V is the volume of solution (mL), M is the weight of adsorbent used per litre of solution (g.L^{-1}),

q (mg. g^{-1}) is the amount of adsorbate retained at time t, and α and k_b are constants [2]. Through the straight-line plot of $loglog\left(\frac{C_0}{C_0 - qM}\right)$ as a function of $log(t)$, the constants α and $k_b$can be determined from the slope and intercept, respectively. If the double logarithmic plots show a linear plot, then the diffusion of adsorbate into the pores of adsorbents is not the only rate-controlling step [3].

The Boyd kinetic model can be expressed by the eqs. S9, S10 and S11 [2,4]:

$$F = \frac{q}{q_e} = 1 - \frac{6}{\pi^2}\sum_{n\_=1}^{\infty}\frac{1}{n^2}exp(-n^2 B_t) \quad \text{(eq. S9)}$$

$$B_t = (\sqrt{\pi} - \sqrt{\pi - \left(\frac{\pi^2 F}{3}\right)} \quad \text{for F < 0.85} \quad \text{(eq. S10)}$$

$$B_t = -0.4977 - \ln(1 - F) \quad \text{for F > 0.85} \quad \text{(eq. S11)}$$

where F is the fraction of contaminant adsorbed at any time compared with the equilibrium. The Boyd kinetic equation is applied to identify the rate-limiting step of the adsorption process. The limiting step is represented by plotting B_t as a function of t. If the plot is linear and passes through the origin, the adsorption process is controlled by intraparticle diffusion [4]. Otherwise, the adsorption process is controlled by film diffusion or by both film and intraparticle diffusions [2,4,5].

The adsorption kinetic parameters of tetracycline (TC), during the first adsorption cycle onto TiO_2_EtOH adsorbent are summarized in Table S1 for the pseudo-first-order, pseudo-second-order and Elovich models, as well as in Table S2 for the the intraparticle diffusion, Bangham and Boyd models.

Table S1 – Adsorption kinetic parameters of TC onto TiO_2_EtOH adsorbent for the pseudo-first-order, pseudo-second-order and Elovich models*.

Model	Parameters						
	q_e^{exp} $(mg.g^{-1})$	q_e^{calc} $(mg.g^{-1})$	k_1 (min^{-1})	R^2	k_2 $(g.mg^{-1}.min^{-1})$	a_e $(mg.g^{-1}.min^{-1})$	b_e $(g.mg^{-1})$
Pseudo-first-order	34.2	27.78	0.017	0.97	-	-	-
Pseudo-second-order	34.2	35.88	-	0.98	0.0015	-	-
Elovich	34.2	-	-	0.95	-	3.99	0.14

* q_e^{exp} and q_e^{calc} represent the experimental and calculated quantities of TC adsorbed at the equilibrium time ($mg.g^{-1}$), respectively; k_1 stands for the pseudo-first-order rate constant of TC sorption (min^{-1}); R^2 is the correlation coefficient; k_2 is the pseudo−second-order adsorption rate ($g.mg^{-1}.min^{-1}$); a_e is the initial sorption rate constant ($mg.g^{-1}.min^{-1}$) and b_e is related to the extent of surface coverage and the activation energy for chemisorption ($g.mg^{-1}$)[2].

Table S2 – Adsorption kinetic parameters of TC onto TiO_2_EtOH adsorbent for the intraparticle diffusion, Bangham and Boyd models*.

Model	Parameters											
	k^1_{id}	C^1	R^2_1	k^2_{id}	C^2	R^2_2	k^3_{id}	C^3	R^2_3	R^2_B	α	k_b
Intraparticle diffusion	3.70	0	1	2.20	7.65	0.86	0.84	21.31	1	-	-	-
Bangham	-	-	-	-	-	-	-	-	-	0.95	0.37	12.09
Boyd	-	-	-	-	-	-	-	-	-	0.98	-	-

* $k^{1,2,3}_{id}$ is the intraparticle diffusion rate constant of the 1st, 2nd and 3rd stages, respectively ($mg.g^{-1}.min^{-0.5}$); C^1, C^2 and C^3 are the values of the intercept of the 1st, 2nd and 3rd stages, respectively ($mg.g^{-1}$); α and k_b ($mg.g^{-1}.min^{-1}$) are the constants from Bangham's model equation, and R^2_B is the correlation coefficient for the Bangham or Boyd model [2].

Figure S5 shows the plot of the intraparticle diffusion model for the adsorption of tetracycline (first cycle) onto TiO_2_EtOH nanopowder.

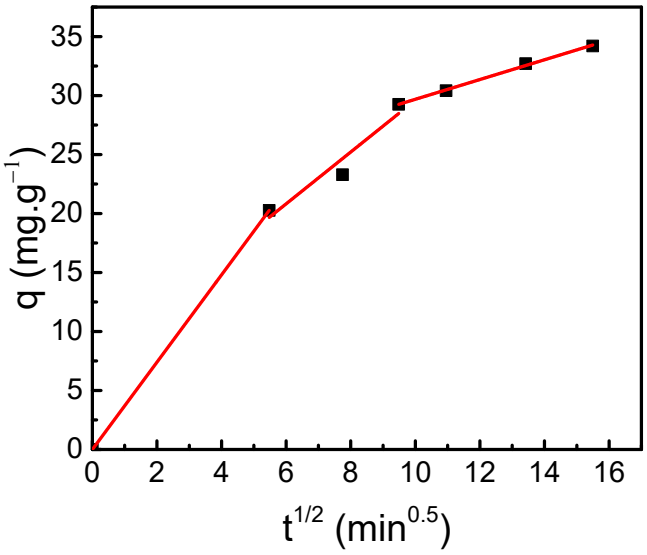

Figure S5 - Plot of the intraparticle diffusion model for the adsorption of tetracycline (first cycle) onto TiO_2_EtOH nanopowder. The solid red line represents the linear fit, while the black squares are the experimental data.

Figure S6 shows the plot of the Bangham's model for the adsorption of tetracycline (first cycle) onto TiO_2_EtOH nanopowder.

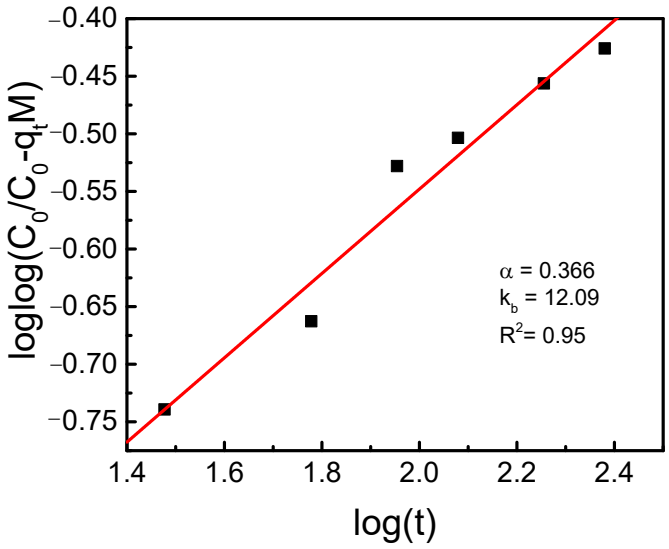

Figure S6 - Plot of Bangham model for the adsorption of tetracycline (first cycle) onto TiO_2_EtOH nanopowder. The solid red line represents the linear fit, while the black squares are the experimental data.

Figure S7 shows the plot of Boyd's model for the adsorption of tetracycline (first cycle) onto TiO_2_EtOH nanopowder.

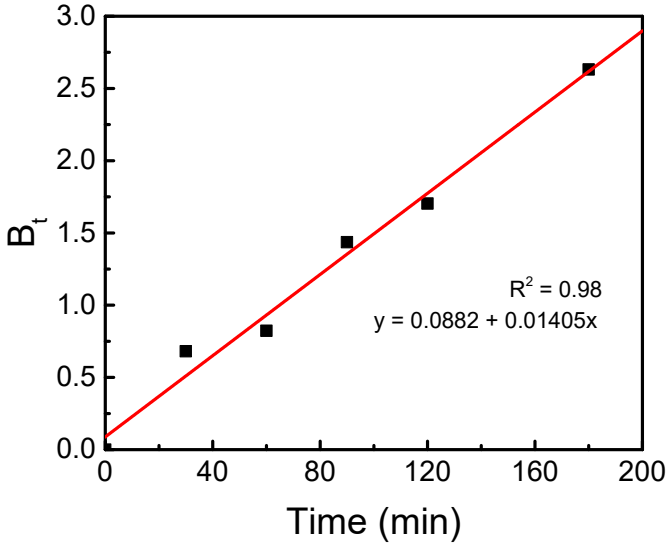

Figure S7 – Plot of Boyd model for the adsorption of tetracycline (first cycle) onto TiO_2_EtOH nanopowder. The solid red line represents the linear fit, while the black squares are the experimental data.

4. Photocatalytic activity of TiO_2 nanopowders for the degradation of tetracycline under solar simulated light

Figure S8 shows the UV-VIS absorption spectra obtained during the photocatalytic degradation of tetracycline (first cycle) under solar simulated light and in the presence of TiO_2 nanopowders synthesized with three different solvents: ethanol, IPA, and water.

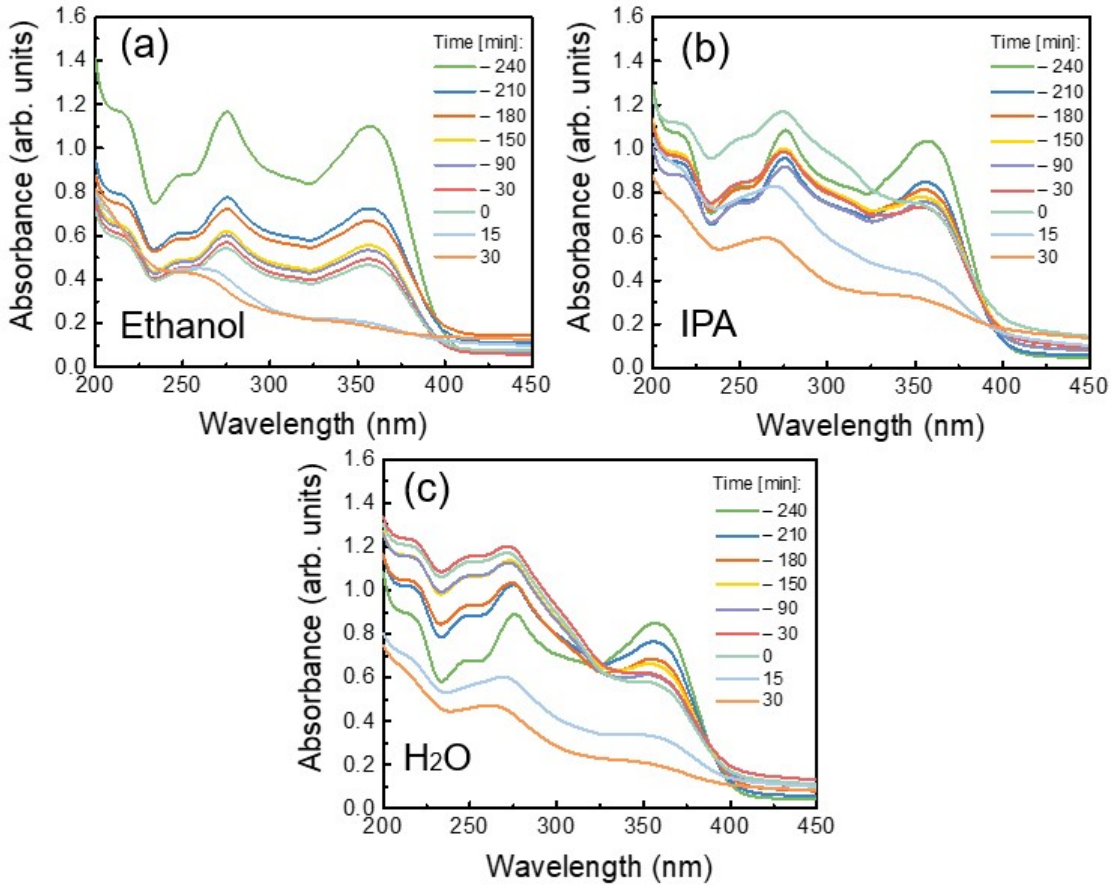

Figure S8 – UV-VIS absorption spectra obtained during the photocatalytic degradation of tetracycline (first cycle) under solar simulating light and in the presence of (a) TiO_2_EtOH, (b) TiO_2_IPA and (c) TiO_2_H_2O nanopowders.

The photocatalytic degradation of tetracycline was estimated by using the pseudo-first-order-kinetics equation based on the Langmuir–Hinshelwood model [6,7]:

$$ln\left(\frac{C}{C_0}\right) = -k_{ap}.t \qquad \text{(eq. S12)}$$

where k_{ap} is the photodegradation apparent rate constant, t is the time, C_0 is the initial concentration and C is the concentration at a certain time. Through the plot of $ln\left(\frac{C}{C_0}\right)$ versus t, the apparent rate constants can be obtained from the slope of the linear regressions [6].

The contribution of different ROS scavengers to the degradation percentage of tetracycline with the TiO_2_EtOH nanopowder under solar simulated light is shown in Figure S9.

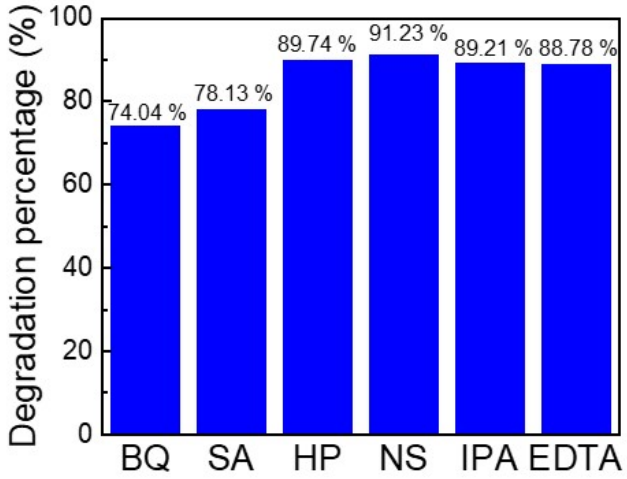

Figure S9 - Degradation percentages (%) of tetracycline with the TiO_2_EtOH nanopowder under solar simulated light, after 240 min of dark, in the presence of different scavengers (p-benzoquinone (BQ), sodium azide (SA), hydrogen peroxide (HP), isopropanol (IPA) and ethylene diamine tetra acetic acid (EDTA) and with no scavenger (NS).

5. Structural characterization of the PU foams

Figure S10 shows the cellular structure of the PU foams. The foam was cut for the observation of its structure.

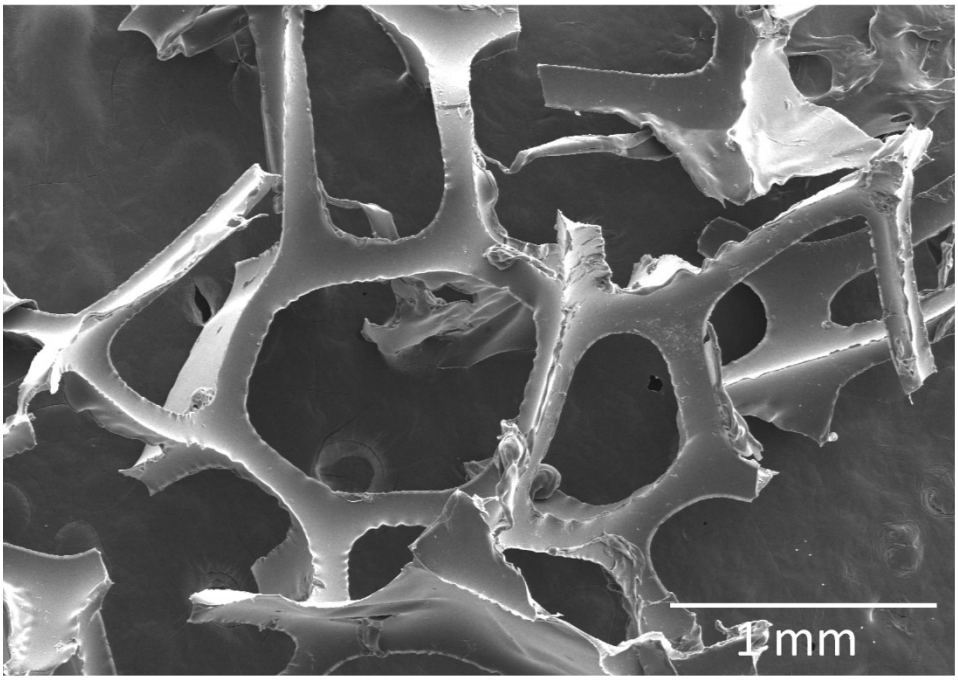

Figure S10 - SEM image of the pristine PU foam.

References

1 H. G. Yang, C. H. Sun, S. Z. Qiao, J. Zou, G. Liu, S. C. Smith, H. M. Cheng and G. Q. Lu, Anatase TiO_2 single crystals with a large percentage of reactive facets,

Nature, 2008, **453**, 638–641.

2 R. Matos, I. Kuźniarska-Biernacka, M. Rocha, J. H. Belo, J. P. Araújo, A. C. Estrada, J. L. Lopes, T. Shah, B. A. Korgel, C. Pereira, T. Trindade and C. Freire, Design and photo-Fenton performance of Graphene/CuS/Fe_3O_4 tertiary nanocomposites for Rhodamine B degradation, *Catalysis Today*, 2023, **418**, 114132.

3 Sumanjit, S. Rani and R. K. Mahajan, Equilibrium, kinetics and thermodynamic parameters for adsorptive removal of dye Basic Blue 9 by ground nut shells and Eichhornia, *Arabian Journal of Chemistry*, 2016, **9**, **2**, S1464–S1477.

4 F. Zamora, E. Sabio, S. Román, C. María González-García and B. Ledesma, Modelling the Adsorption of p-Nitrophenol by the Boyd Method in Conjunction with the Finite Element Method †, *Adsorption Science and Technology*, 2010, **28(8)**, 671–687.

5 C. Yao and T. Chen, A film-diffusion-based adsorption kinetic equation and its application, *Chemical Engineering Research and Design*, 2017, **119**, 87–92.

6 M. L. Matias, M. Morais, A. Pimentel, F. X. Vasconcelos, A. S. Reis Machado, J. Rodrigues, E. Fortunato, R. Martins and D. Nunes, Floating TiO_2-Cork Nano-Photocatalysts for Water Purification Using Sunlight, *Sustainability*, 2022, **14(15)**, 9645.

7 M. L. Matias, A. Pimentel, A. S. Reis-Machado, J. Rodrigues, J. Deuermeier, E. Fortunato, R. Martins and D. Nunes, Enhanced Fe-TiO_2 Solar Photocatalysts on Porous Platforms for Water Purification, *Nanomaterials*, 2022, **12**, Article 1005.